Supporting Information

Enhanced Fe(II)-artemisinin-mediated chemodynamic therapy with efficient Fe(III)/Fe(II) conversion circulation for cancer treatment

Xiao Xu[b], Yun Wang[a], Dan Yan[a], Chunling Ren[a], Yuqian Cai[a], Shanting Liao[b], Lingyi Kong[a,*], Chao Han[a,*]

[a] *Jiangsu Key Laboratory of Bioactive Natural Product Research and State Key Laboratory of Natural Medicines, School of Traditional Chinese Pharmacy, Center for Analysis and Testing, China Pharmaceutical University, 639 Long Mian Avenue, Nanjing 211198, China.*

[b] *Department of Biochemistry and Molecular Biology, School of Medicine, Nanjing University of Chinese Medicine, 138 Xianlin Avenue, Nanjing 210023, PR China*

[*]Corresponding author:

Tel./Fax: +86 25 8327 1405. (Lingyi Kong)

E-mail address: cpu_lykong@126.com (Lingyi Kong), hanchao@cpu.edu.cn (Chao Han).

Supplemental Figures

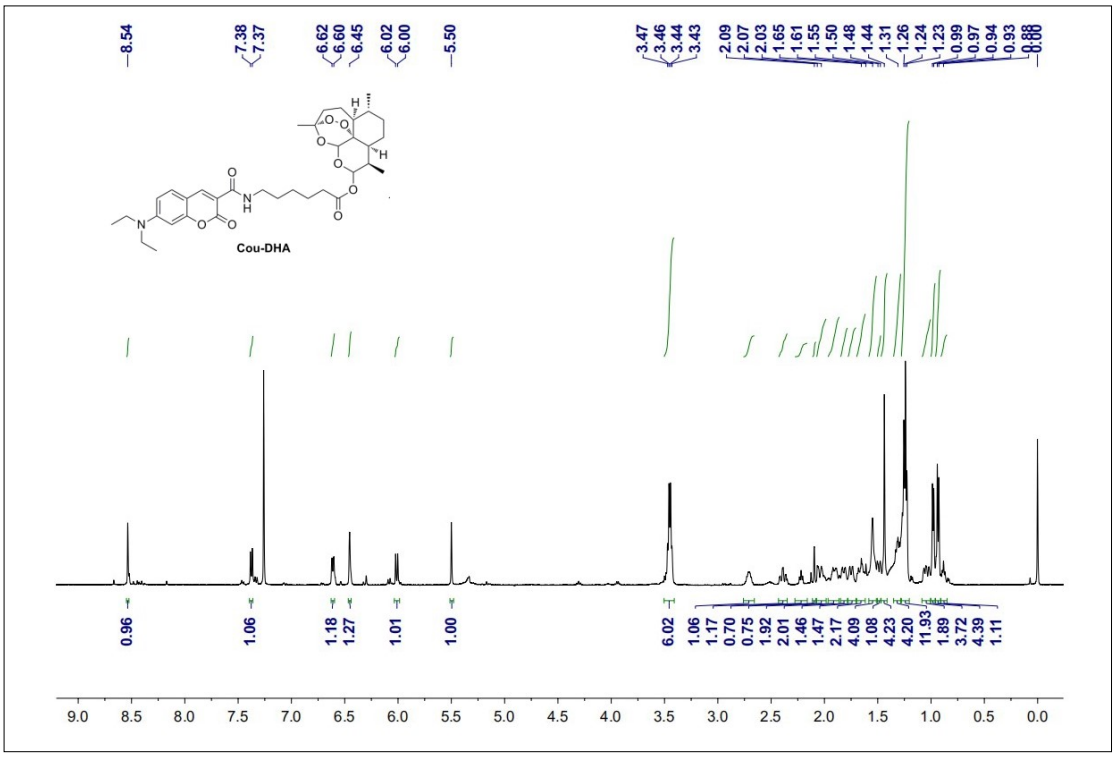

Figure S1. ^{1}H NMR spectrum of Cou-DHA ($CDCl_3$, 500 MHz).

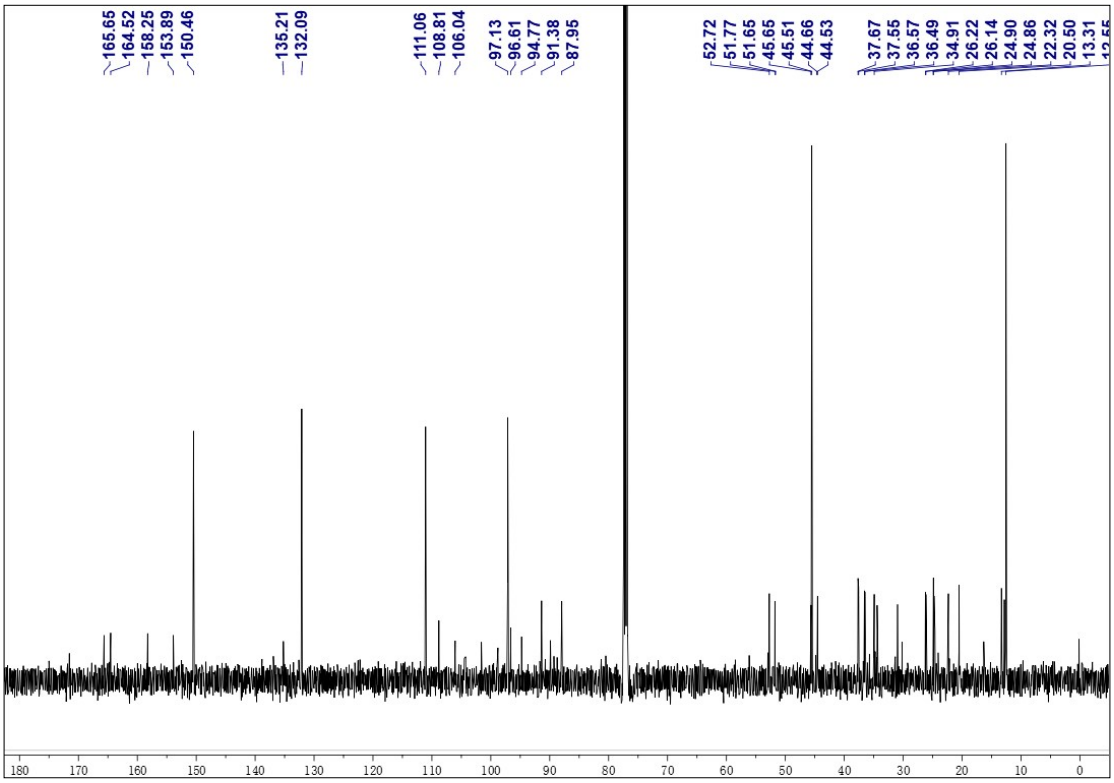

Figure S2. ^{13}C NMR spectrum of Cou-DHA ($CDCl_3$,125 MHz).

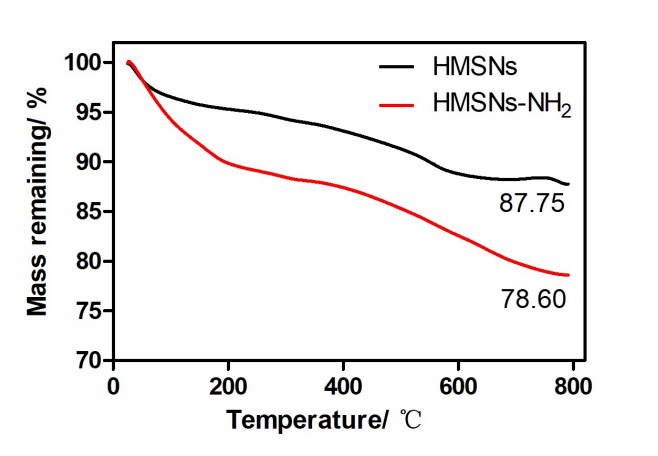

Figure S3. TGA analysis of HMSNs and HMSNs-NH_2.

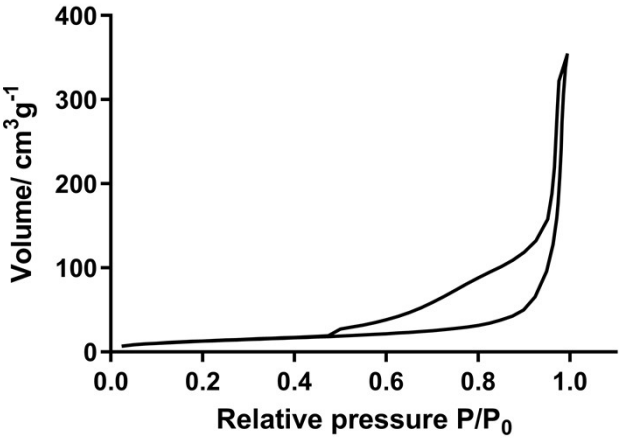

Figure S4. N_2 adsorption-desorption isotherms of HMSNs-NH_2.

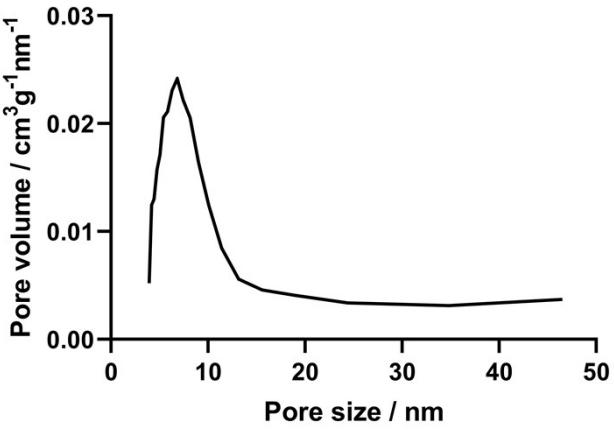

Figure S5. Pore size distribution of HMSNs-NH_2.

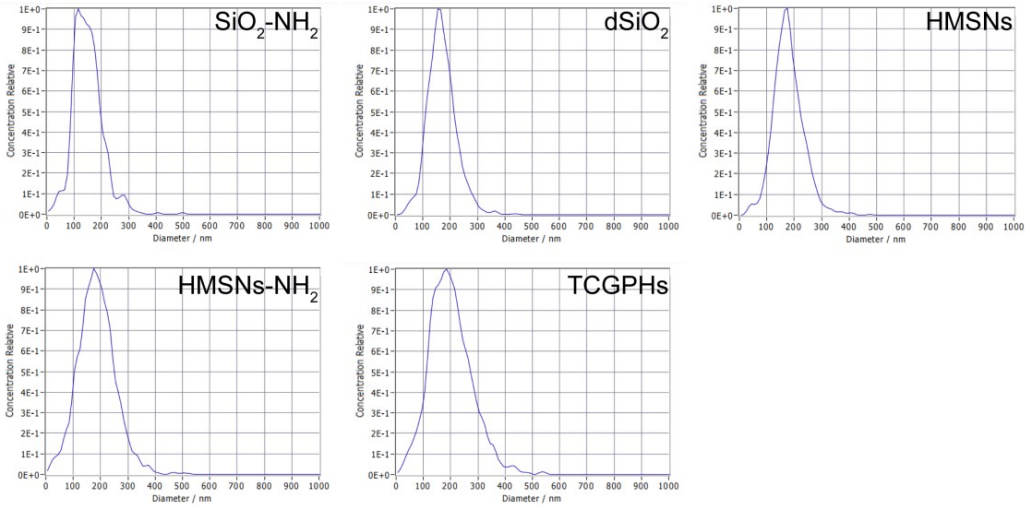

Figure S6. The particle size of SiO_2-NH_2, $dSiO_2$, HMSNs, HMSNs-NH_2, and TCGPHs.

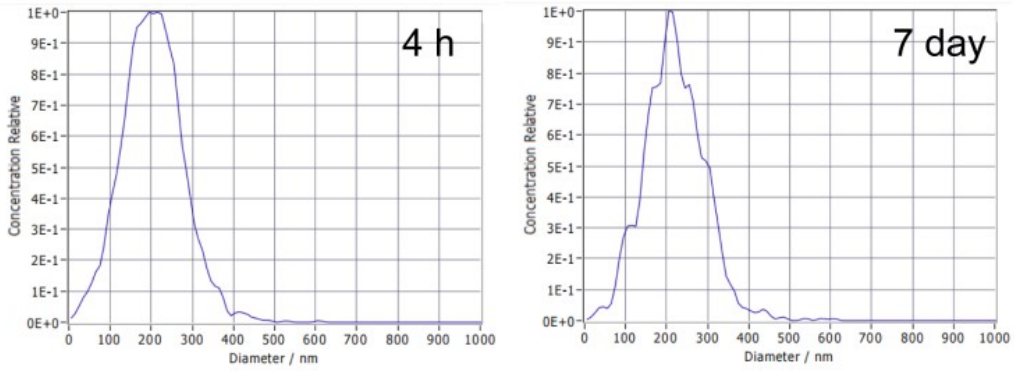

Figure S7. The particle size of TCGPHs in PBS at 4 h and 7 days.

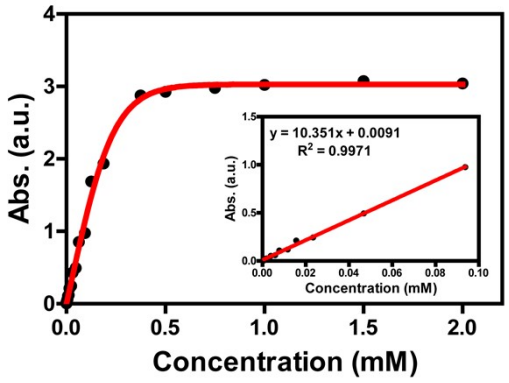

Figure S8. Maximum absorption at ~410 nm of Cou-DHA solutions at various concentrations. Inset: linear concentration range of Cou-DHA (0.0007-0.0938 mM).

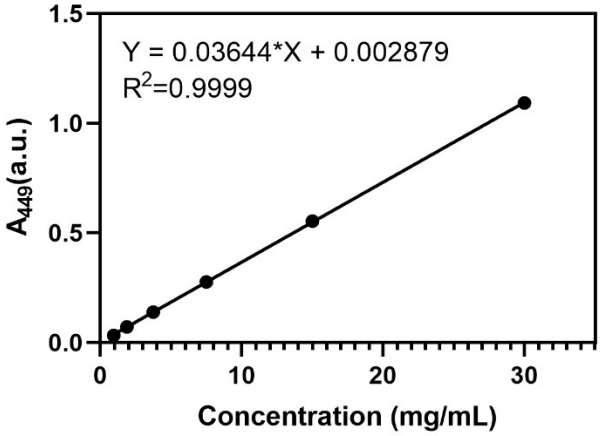

Figure S9. Linear relationships between the UV-vis absorbance intensity at 449 nm and the GOx concentration.

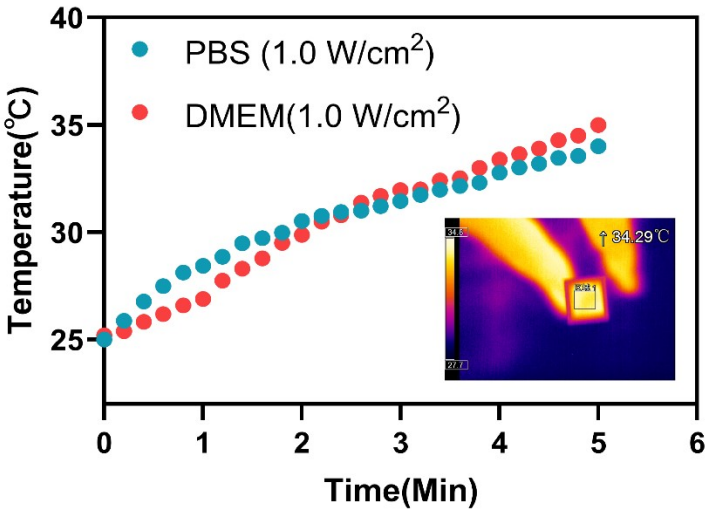

Figure S10. Photo-thermal conversion curves when PBS or DMEM under 980 nm laser irradiation at 1.0 W/cm^2 for 5 min. Inset: Thermal images of PBS solution after NIR laser irradiation at 5 min.

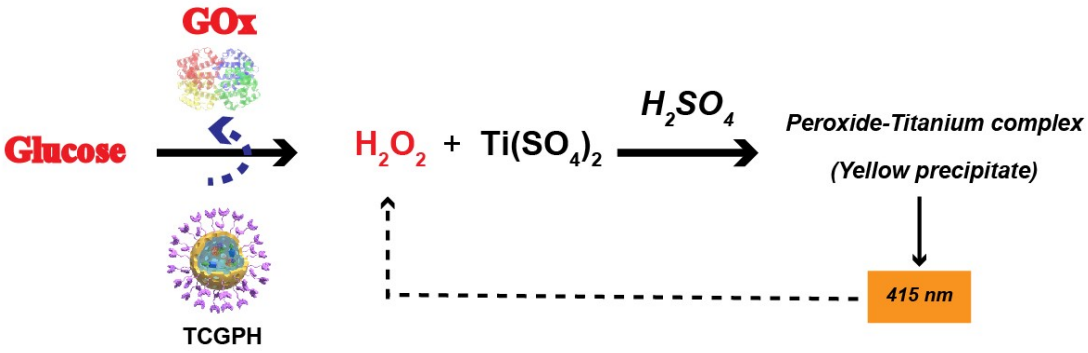

Figure S11. Schematic diagram illustrating the mechanisms of H_2O_2-detection.

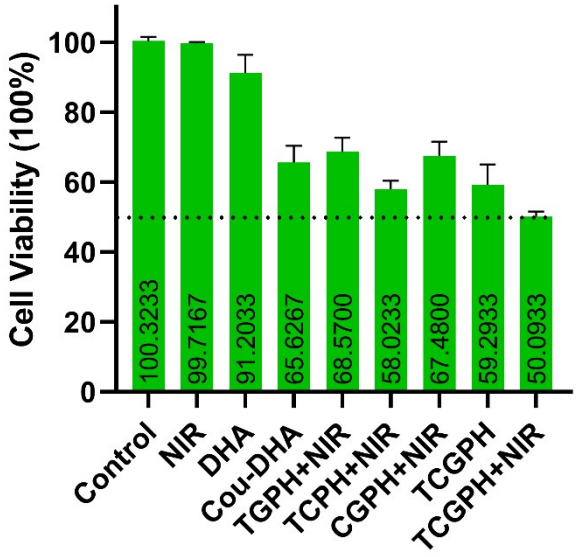

Figure S12. MTT assay of Hela cells with different treatments in the hypoxia environment (***$P < 0.001$, ****$P < 0.0001$).

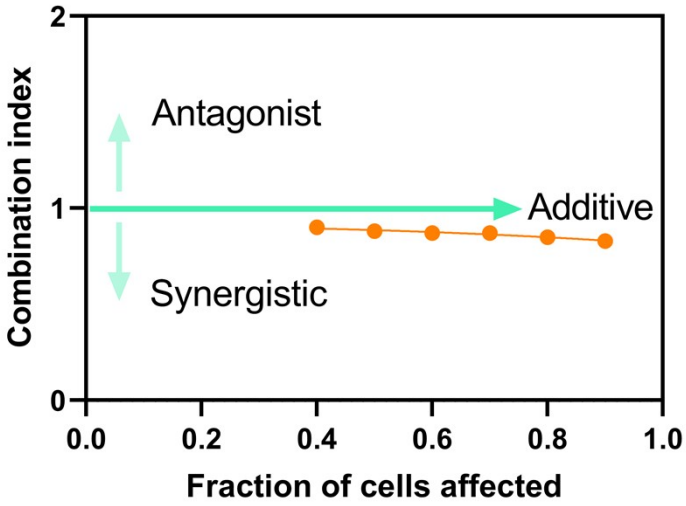

Figure S13. The combination index (CI)-plot of Hela cells calculated by Cou-DHA, TGPH+NIR, and TCGPH+NIR based on MTT assay.

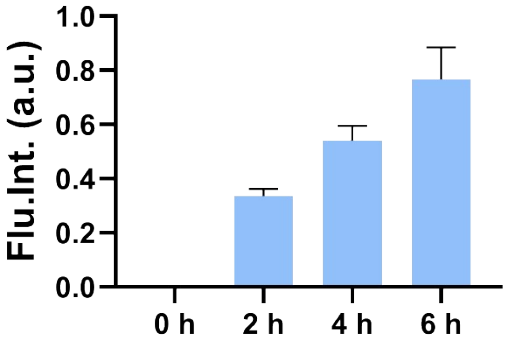

Figure S14. Quantification of fluorescence intensities of TCGPHs during cellular uptake by Hela cell (equivalent DHA concentration of 2 μM).

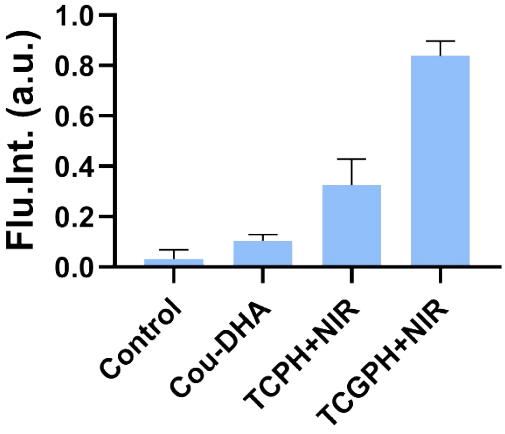

Figure S15. Quantification of fluorescence intensities of Amplex red (H_2O_2 indicator) in Hela cells with different treatments (equivalent DHA concentration of 4 μM, 8 h).

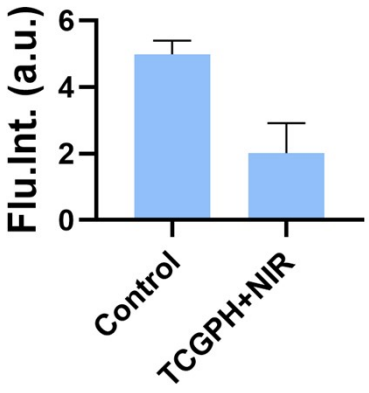

Figure S16. Quantitative fluorescence analysis of Image-iT™ Green Hypoxia Reagent in Hela cells with different treatments in the hypoxia environment (equivalent DHA concentration of 4 μM, 8 h).

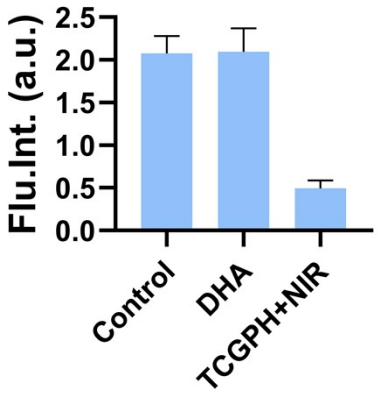

Figure S17. Quantitative immunofluorescence analysis of expression levels of HIF-1α in Hela cells with different treatments in the hypoxia environment (equivalent DHA concentration of 2 μM, 24 h).

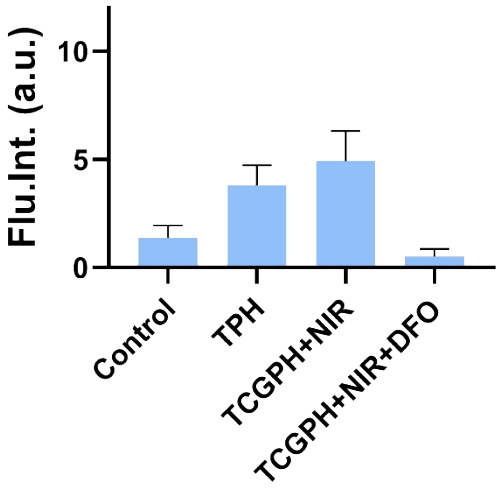

Figure S18. Quantification of fluorescence intensities of FerroOrange (Fe^{2+} indicator) in Hela cells with different treatments (equivalent DHA concentration of 4 μM, 8 h).

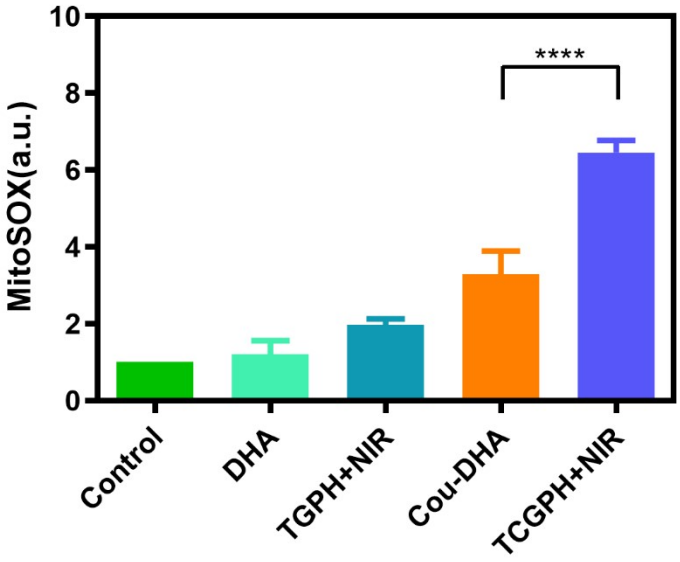

Figure S19. Relative quantification of mitochondrial superoxide levels of Hela cells with different treatments (equivalent DHA concentration of 4 μM, 8 h). Error bars indicate the s.d. (n = 3). ****$P < 0.0001$.

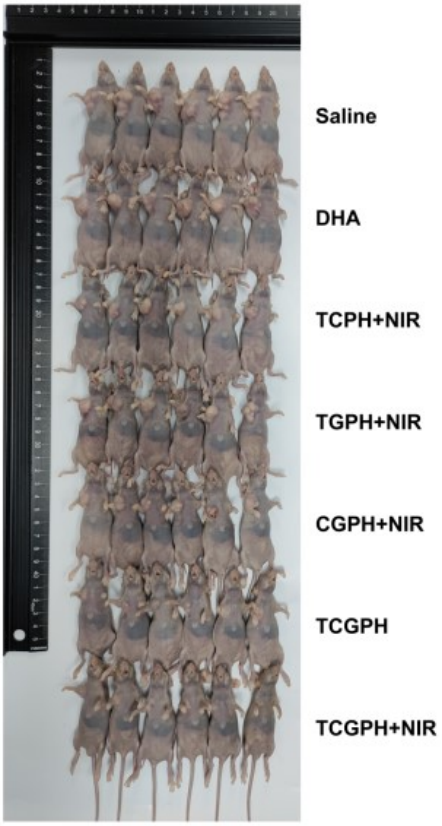

Figure S20. Photograph of Hela tumor-bearing mice after 14-day different treatments.

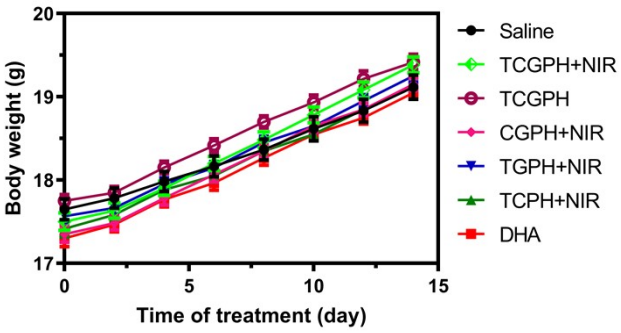

Figure S21. Bodyweight changes in tumor-bearing mice during treatment. Error bars indicate the s.d. (n = 6).

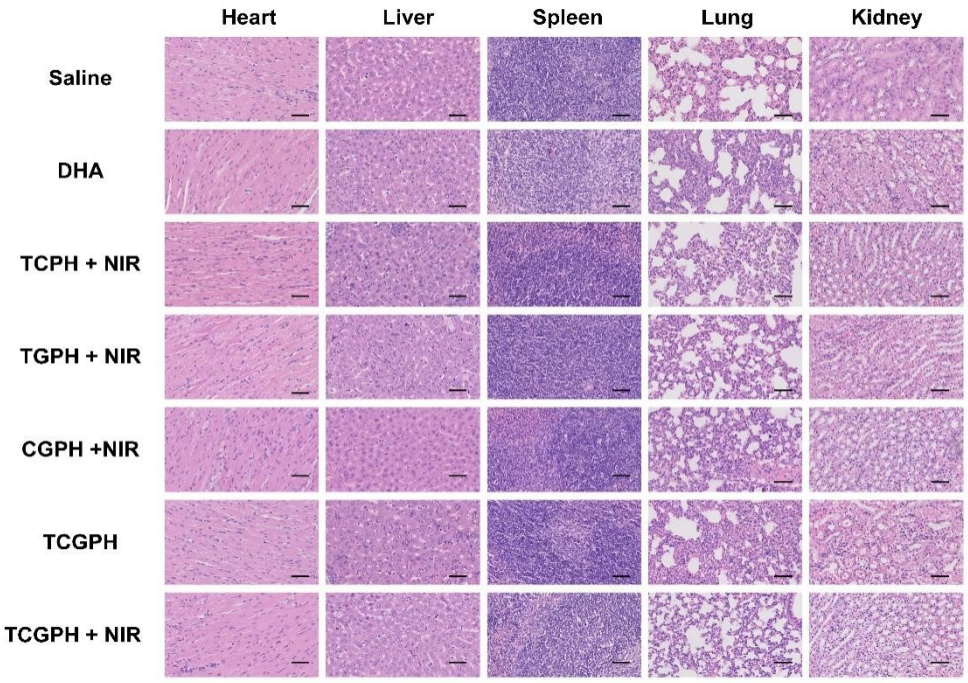

Figure S22. HE staining of organs, including heart, liver, spleen, lung, and kidney from mice after different treatments. Scale bars: 50 μm.

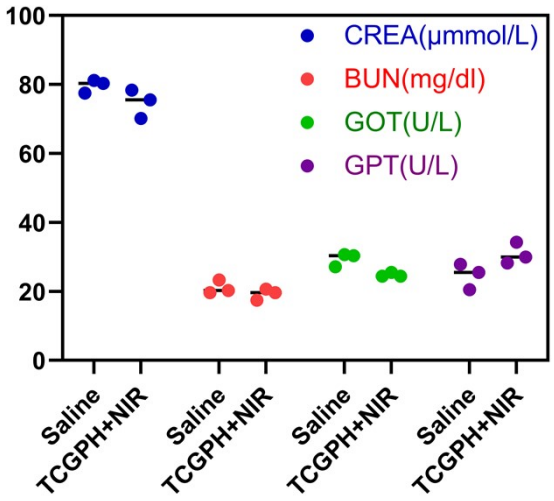

Figure S23. Blood biochemistry tests of CREA, BUN, GOT, and GPT following treatments. (n = 3).

Table 1. The abbreviations of different nanoformulations.

Abbreviation	Full title
HMSN	Hollow mesoporous silica nanoparticle
TCGPH	Tf-HMSNs@Cou-DHA/GOx/PFP
TCGH	Tf-HMSNs@Cou-DHA/GOx
TGPH	Tf-HMSNs@GOx/PFP
CGPH	HMSNs@Cou-DHA/GOx/PFP
TCPH	Tf-HMSNs@Cou-DHA/PFP
TPH	Tf-HMSNs@PFP